Desalination and Water Treatment
www.deswater.com

doi: 10.5004/dwt.2022.28656

266 (2022) 226–235
August

Assessment of photocatalytic n-TiO_2/UV and n-TiO_2/H_2O_2/UV methods to treat DB 86, RY 145 and AV 90 dye mix containing wastewater

Meryem Aksu[a,*], Muhammed Has[a], N. Pınar Tanattı[b], Büşra Erden[a], Gamze Katırcıoğlu Sınmaz[a], Füsun Boysan[a], İ. Ayhan Şengil[a]

[a]*Environmental Engineering Department, Sakarya University, 54100 Sakarya-Turkey, Tel. +90 264 295 5485; Fax: +90 264 2955601; email: meryemm@sakarya.edu.tr (M. Aksu)*
[b]*Department of Environmental Protection Technologies, Sakarya University of Applied Sciences, Turkey, 54100 Sakarya-Turkey*

Received 28 December 2021; Accepted 31 May 2022

ABSTRACT

This study examined and compared the n-TiO_2/H_2O_2/UV and n-TiO_2/UV processes to remove the content of synthetic wastewater containing Direct Blue (DB86), Reactive Yellow (RY145) and Acid Violet (AV90) dye mix. The optimum parameters for both processes have been determined as pH 3, 125 mg/L n-TiO_2 and 45 min, and the H_2O_2 dose has been specified as 750 mg/L in the n-TiO_2/H_2O_2/UV process. While the removal efficiencies were 54.38% at 436 nm, 44.20% at 525 nm and 85.72% at 620 nm for the n-TiO_2/UV process, 90.63% at 436 nm, 92.27% at 525 nm and 99% at 620 nm were obtained for n-TiO_2/H_2O_2/UV process. With H_2O_2 addition to the process, treatment efficiencies have been increased drastically. Moreover, due to the results of the kinetic analyses for both processes, the pseudo-second-order was observed to be the most appropriate kinetic model, depending on the regression coefficient in color removal.

Keywords: Direct Blue (DB86); Reactive Yellow (RY145); Acid Violet (V90); n-TiO_2/H_2O_2/UV; n-TiO_2/UV

1. Introduction

The textile industry is one of the oldest sectors, and the dimensions of the sector are expanding day by day due to the increasing population [1]. The total budget of the global textile industry has been estimated to be 920 billion USD. Until 2024 it has expected to reach 1,230 billion USD [2]. Despite the economic contribution of the textile industry, textile production contributes the environmental pollution, with the usage of vast amounts of water, fuel and chemicals [3].

Textile industry wastewaters include a mixture of dyes and a variety of chemicals [4]. Dyes are one of the larger groups of pollutants in wastewater released from textile industries. Discharged dyes to water bodies prevent light penetration and disturb aquatic life [5]. According to the application types, the dyestuffs are classified as reactive dyes, disperse dyes, acid dyes, basic dyes, direct dyes, and vat dyes [6,7]. Most of the dyestuffs used are toxic, non-biodegradable and carcinogenic, and direct discharge to the receiving environment is hazardous for the environment and human health [8]. Many methods have been used in the literature to degrade textile dyestuffs and the purification of water.

In studies on the degradation of Direct Blue 86, Reactive Yellow 145 and Acid Violet 90 dyes (O_3 and O_3/UV), photocatalytic oxidation [9,10], adsorption [11–14], coagulation [15], persulfate degradation [16], electrocoagulation [17] methods were observed.

Within the scope of this study, the treatment of synthetic wastewater samples containing 150 mg/L dyestuffs (DB 86, RY 145 and AV 90 50 mg/L each) with n-TiO_2/UV

* Corresponding author.

and n-TiO_2/H_2O_2/UV processes was investigated. Although there are limited studies on the removal of these dyes in the literature, textile wastewater contains dyestuff mixtures.

Depending on the product and dye variety, textile industry wastewater contains a mixture of many dyes. For this reason, the sector demands to perform the removal of the mixed dyes used, rather than the removal of a single dye. In our study, the efficient removal of three different dye mixtures with the specified methods was investigated in a way that would meet the needs of the factory in which the dyes were supplied. Due to the carcinogenic, mutagenic and toxic properties of dyes used in the textile industry, it holds great importance to treat them in accordance with discharge regulations

In this context, this study is an original contribution to the literature by investigating the treatment of synthetic wastewater containing three different dyestuffs by the n-TiO_2/H_2O_2/UV and n-TiO_2/UV processes. In both processes, pH (3–11), n-TiO_2 dose 25–150 mg/L, and reaction time 5–60 min parameters were studied. For the n-TiO_2/H_2O_2/UV process, the H_2O_2 dose 250–1,500 mg/L parameter was also examined. By using all these parameters, the effects of the processes on the color removal were evaluated in the synthetic wastewater sample containing the mixture of three different dyestuffs (DB 86, RY 145, AV 90) in equal amounts.

2. Materials and methods

2.1. Materials

Direct Blue 86 (DB 86), Reactive Yellow 145 (RY 145) and Acid Violet 90 (AV 90) dyestuffs were provided from a textile factory in Sakarya. Hydrochloric acid (HCl) and sodium hydroxide (NaOH) at brand MERCK has been used to adjust the pH of the solutions. pH measurements have been performed pH meter at brand HANNA. Magnetic stirrers at brand MTOPS and NUVE brand centrifuge device has been used to remove n-TiO_2. 21 nm diameter n-TiO_2 was used as a catalyst at brand SIGMA ALDRICH. The diameter of commercially available n-TiO_2 was determined as 21 nm from the scanning electron microscopy (SEM) images given in Fig. 1. It can be seen clearly from the SEM image, n-TiO_2 that was used in the experiment has a homogeneous structure. Dye mix concentrations have been measured with a Pharo 3600 spectrophotometer at brand MERCK. Zeta potential analyses have been measured with the Zeta sizer brand Nano-ZS model device.

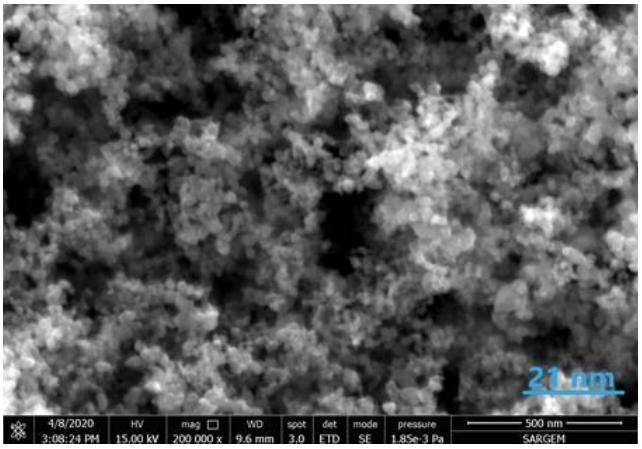

Fig. 1. SEM image for n-TiO_2.

2.2. Dyestuff mixture preparation and color measurement method

In this study, synthetic wastewater was prepared by mixing DB 86, RY 145, and AV 90 (each 50 mg/L) dyestuffs with the total 150 mg/L initial concentration. The color limit values according to European norms are given in Table 1. The initial values according to European norms in synthetic water containing dyestuffs used in the experiments are given in Table 2. Experiments were repeated three times, and the samples were centrifuged at 4,500 rpm for 15 min before each measurement for the removal of TiO_2 nanoparticles used. Color measurements were performed as EN ISO 7887-B. According to the method, the color is specified with measurements of attenuation of light absorption by using a spectrophotometer at a minimum of three different wavelengths. The measurements were performed with 436, 525 and 620 nm wavelengths of the visible spectrum with a 50 mm optical pathlength cell [18].

2.3. Reactor design

The reactor design of the n-TiO_2/UV and n-TiO_2/H_2O_2/UV processes used in color removal experiments is shown in Fig. 2. A photoreactor consisting of six pieces of 6-W lamps with a wavelength of 254 nm was used for the photocatalytic oxidation experiment. A cylindrical sample container made of quartz glass with a volume of 140 mL was used inside the reactor. A homogeneous mixture was achieved by placing the reactor on the magnetic stirrer. In order to keep the system temperature constant, a pump is used to provide cold air to the system.

2.4. Photocatalytic reactions

Various methods such as ozonation, irradiation, H_2O_2, and oxidation are used for the treatment of dye wastewater [19,20]. Due to the non-toxic, insoluble, inexpensive and highly reactive nature of TiO_2, it has been used to treat wastewater containing TiO_2/UV dyes. The purification mechanism of TiO_2 is given in Eqs. (1)–(3) [21].

$$TiO_2 + h_v \rightarrow e^-_{CB} + h^+_{VB} \quad (1)$$

Table 1
European norm color limit values

436 nm	525 nm	620 nm
7 m^{-1}	5 m^{-1}	3 m^{-1}

Table 2
Initial color values of synthetic wastewater of dye mix

436 nm	525 nm	620 nm
32 m^{-1}	36.2 m^{-1}	30.1 m^{-1}

$$h^+_{VB} + OH^- (surface) \rightarrow OH^\bullet \quad (2)$$

$$h^+_{VB} + H_2O \rightarrow OH^\bullet + H^+ \quad (3)$$

where hυ represents UV radiation; h^+_{VB} is valence-band holes; e^-_{CB} is conduction-band electrons.

The $OH^\bullet$ radical, which provides the removal of pollutants, can occur in various forms, as seen in the equations. Electrons that emerge as a result of photon irritation can interact with other molecules as well as release heat by interacting with valence-band holes. These holes can provide oxidation by direct electron transfer. The mechanism of the n-TiO_2/H_2O_2/UV photocatalytic treatment system is briefly shown by the Eqs. (4)–(8) [21–23];

$$Dye + h_v \rightarrow products \quad (4)$$

$$H_2O_2 + h_v \rightarrow 2OH \quad (5)$$

$$Dye + {}^\bullet OH \rightarrow products \quad (6)$$

$$e^-_{CB} + O_2 \rightarrow O_2^- \quad (7)$$

$$e^-_{CB} + h^+_{VB} \rightarrow heat \quad (8)$$

where h_v represents UV radiation; h^+_{VB} is valence-band holes; e^-_{CB} is conduction-band electrons.

3. Results and discussion

3.1. Effect of pH on color removal

The pH parameter affects the removal efficiency for dye removal in wastewater containing dyestuffs [24]. The experiments were carried out at pH 3, 5, 9 and 11 to investigate the effects of pH on TiO_2/UV and TiO_2/H_2O_2/UV processes for dye removal efficiency. In the beginning, synthetic textile wastewater with a total dye concentration of 150 mg/L was prepared, with 50 mg/L of each of three dyes. The initial color values of the Direct Blue 86, Reactive Yellow 145, and Acid Violet 80 dye mixture measured as 32 m^{-1} at 436 nm, 36.2 m^{-1} at 525 nm and 30.1 m^{-1} at 620 nm. The experiments have been performed with 100 mg/L n-TiO_2 dose, 30 min reaction time and 36 W light intensity to investigate the optimum pH value for both TiO_2/UV and TiO_2/H_2O_2/UV processes. Additionally, 1,000 mg/L H_2O_2 was used in the TiO_2/H_2O_2/UV process. The effect of pH on the color removal efficiency in photocatalytic processes using n-TiO_2 and photocatalytic processes with H_2O_2 is given in Fig. 3.

$$TiO_2 e^-_{(CB)} + H_2O_2 \rightarrow TiO_2 + {}^\bullet OH + OH^- \quad (9)$$

$$H_2O_2 \rightarrow {}^\bullet OH + {}^\bullet OH \quad (10)$$

$$H_2O_2 + O_2^{\bullet -} \rightarrow {}^\bullet OH + H^+ + O_2 \quad (11)$$

$$H_2O_2 + {}^\bullet OH \rightarrow HO_2^\bullet + H_2O \quad (12)$$

$$HO_2^\bullet + {}^\bullet OH \rightarrow HO_2^\bullet + H_2O \quad (13)$$

As can be seen in Fig. 3, the color removal efficiency decreases with the increase in pH in the n-TiO_2/UV and n-TiO_2/H_2O_2/UV processes. The highest color removal efficiency is obtained at pH 3 in both processes. Color removal efficiencies show a decreasing trend with the increase in

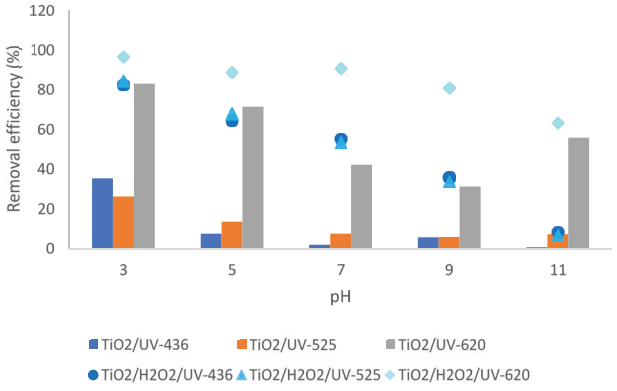

Fig. 3. Effect of pH on the color removal ($C_{o,436\ nm}$ = 32 m^{-1}; $C_{o,525\ nm}$ = 36.2 m^{-1}; $C_{o,620\ nm}$ = 30.1 m^{-1}; n-TiO_2 dose = 100 mg/L; H_2O_2 dose = 1,000 mg/L; t = 30 min).

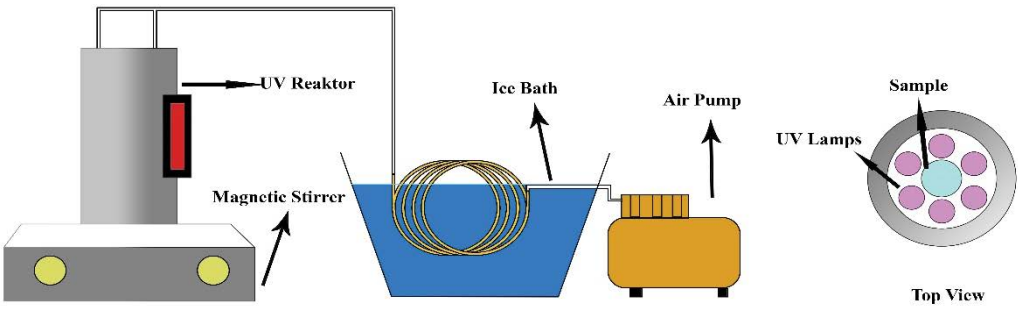

Fig. 2. Experimental set-up.

pH. Therefore, the optimum pH was determined as 3 in both processes. Although the pH decrease in both processes increases the color removal efficiency, it has also been observed that the n-TiO_2/H_2O_2/UV process has better removal performance. Unlike the n-TiO_2/UV process, in the n-TiO_2/H_2O_2/UV process, with the addition of H_2O_2 formation of $OH^{\bullet}$ radicals multiply and correlatively the oxidation capacity increases [25].

In the n-TiO_2/UV process, the color removal efficiencies for 436, 525 and 620 nm at pH 3 are 35.31%, 26.24% and 83.06%, respectively, while in the n-TiO_2/H_2O_2/UV process, the removal efficiencies at the same wavelengths are 82.5%, 84.53% and 96.35%, respectively. When the situation at pH 3 is examined for both processes, the difference in color removal efficiency is approximately 48% at 436 nm, approximately 58% at 525 nm and approximately 13% at 620 nm. In the literature, n-TiO_2/UV and n-TiO_2/H_2O_2/UV processes have been used for color removal using different azo dyes, and dye removal has been achieved with the highest efficiency in acidic conditions. In these studies, high color removal was found between pH 2.5 and 4.5 [26–28].

In the literature, TiO_2 catalysed photocatalytic studies are examined, and the dye removal efficiency is generally high at acidic pHs. As a result of the positive charge of the surface of TiO_2 in an acidic solution, it absorbs negatively charged organic compounds. Therefore, high photocatalytic activity is expected to occur [29]. The zeta potential of the catalysts varies depending on the pH of the solution [30]. The zeta potential change of n-TiO_2 used in the experiments depending on pH is given in Table 3. Table 3 shows, while the zeta potential of TiO_2 is high at low pH, it decreases as the pH rises and even becomes negative at high pH. The zero point of charge for n-TiO_2 is at an almost neutral pH. The TiO_2 surface is positively charged below approximately neutral pH; however, the particle surface becomes negatively charged above neutral pH [31].

3.2. Effect of catalyst dose on color removal

The catalyst dose is one of the essential parameters in photocatalytic processes [32]. Since TiO_2 is a low cost, nontoxic, easy to procure material, has been prefered catalyst used in heterogeneous photocatalytic processes [33]. The particle size, shape, and crystal structure of TiO_2 are suitable for changes at the desired level in order to increase the degradation rate and amount of the substances desired to be purified in photocatalytic processes [34].

In this study, studies have been taken place in the range of 25–150 mg/L TiO_2 dose to examine the effect of catalyst dose on color removal in synthetic wastewater containing dyestuff (DB 86, RY 145, AV 90). The effect of catalyst dose on color removal is seen in Fig. 4. In the n-TiO_2/UV process, color removals have been obtained as 13.44% at 436 nm, 16.02% at 525 nm and 50.17% at 620 nm at a dose of 25 mg/L n-TiO_2. In this process, color removal efficiencies at 150 mg/L n-TiO_2 doses were 43.44% at 436 nm, 32.87% at 525 nm and 83.39% at 620 nm. In the n-TiO_2/H_2O_2/UV process, color removals have been achieved as 51.56%, 65.75% and 79.40% at 436, 525 and 620 nm for 25 mg/L n-TiO_2 dose, meanwhile at 436, 525 and 620 nm for 150 mg/L n-TiO_2 dose removal efficiencies were 89.38%, 92.54% and 98.01% respectively. While the color removal increases with the increase of the catalyst dose, there is no high increase in color removal after 125 mg/L n-TiO_2 dose, therefore 125 mg/L has been determined as optimum n-TiO_2 dose. Similarly, in the study of Amoli et al., the photocatalytic degradation of synthetic wastewater containing Direct Blue 199 and Basic Yellow 28 was investigated, and with the increase of the TiO_2 dose, the removal efficiency of the dyestuffs increased up to a certain point, but then a considerable increase was not observed [35]. The reduction in removal efficiency at a very high catalyst dose may be due to the low transmittance of the reaction mixture and light scattering. Another reason is thought to be the deactivation of reactive molecules, which may occur due to collision with non-reactive molecules [32]. As the amount of catalyst used increases, the contact surface area increases, and the treatment efficiency generally increases because it creates more catalyst active sites for the substances intended to degrade [36,37].

Table 3
Zeta potentials of n-TiO_2 depending on the pH

pH	Zeta potential (mV)
2	2.61
3	1.388
5	0.691
7	0.218
9	–3.33

3.3. Effect of H_2O_2 dose on color removal

Experiments have been performed at pH 3, 125 mg/L n-TiO_2 dose, 30 min reaction time and 36 W light intensity while examining the effect of H_2O_2 dose on color removal in n-TiO_2/H_2O_2/UV process. It is known that the $OH^{\bullet}$ radicals formed when H_2O_2 is added cause the removal of dyestuffs, and the effect of H_2O_2 on color removal efficiencies has been investigated between 250–1,500 mg/L of H_2O_2 doses and has been shown in Fig. 5. While color removal is fewer at 250 mg/L H_2O_2 dose, the increase in color removal is slightly

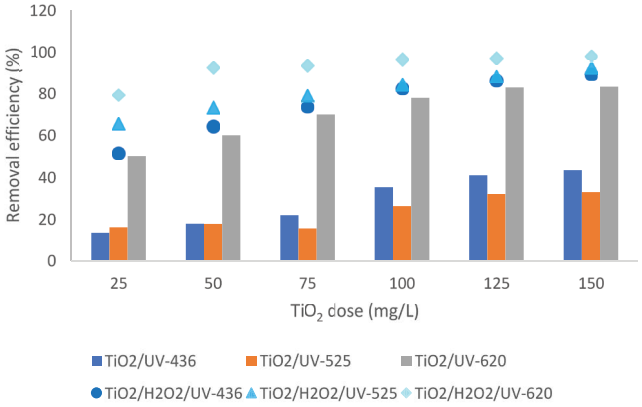

Fig. 4. Effect of n-TiO_2 dose on the color removal ($C_{o,436\,nm}$ = 32 m^{-1}; $C_{o,525\,nm}$ = 36.2 m^{-1}; $C_{o,620\,nm}$ = 30.1 m^{-1}; pH = 3; H_2O_2 dose = 1,000 mg/L; t = 30 min).

raised up after 750 mg/L H_2O_2 dose, though H_2O_2 dose does not affect color removal at 620 nm, only around 2%. On the contrary, the effect of H_2O_2 dose on color removal at 436 nm and 525 nm is quite evident. Color removals at 750 mg/L have been achieved as 85.63% at 436 nm, 86.74% at 525 nm and 97.34% at 620 nm.

Due to the rise in H_2O_2 dose, Chu also stated that treatment efficiencies are affected by the autodegradation of H_2O_2 and the reaction of hydroxyl radicals with excessive H_2O_2 concentrations [38]. This can be explained as the reason why the increase in removal efficiency slows down after 750 mg/L.

3.4. Effect of reaction time on color removal

In order to investigate the effect of reaction time on color removal from synthetic wastewater samples containing dyes in n-TiO_2/UV and n-TiO_2/H_2O_2/UV processes, pH 3, 125 mg/L n-TiO_2 dose and 36 Watt light intensity conditions have been studied. Furthermore, 750 mg/L H_2O_2 was used for the n-TiO_2/H_2O_2/UV process. Fig. 6 shows the effect of reaction time on color removal in both processes. According to

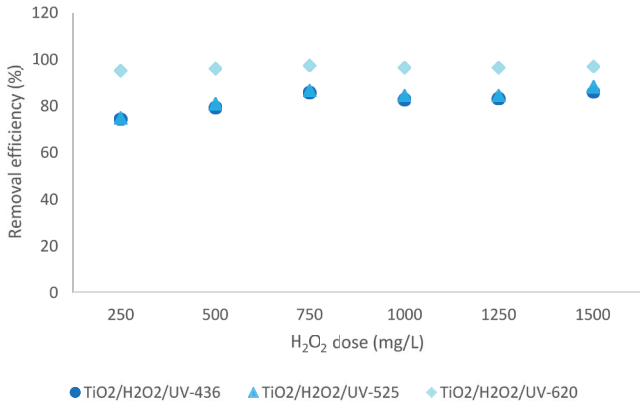

Fig. 5 Effect of H_2O_2 dose on the color removal ($C_{o,436\,nm}$ = 32 m^{-1}; $C_{o,525\,nm}$ = 36.2 m^{-1}; $C_{o,620\,nm}$ = 30.1 m^{-1}; pH = 3; n-TiO_2 dose = 125 mg/L; t = 30 min).

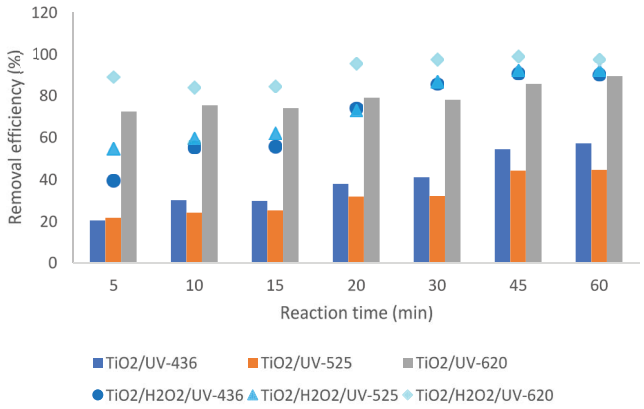

Fig. 6 Effect of reaction time on the color removal ($C_{o,436\,nm}$ = 32 m^{-1}; $C_{o,525\,nm}$ = 36.2 m^{-1}; $C_{o,620\,nm}$ = 30.1 m^{-1}; pH = 3; n-TiO_2 dose = 125 mg/L; H_2O_2 dose = 750 mg/L).

Fig. 6, color removal increased until the 45th min and then the increase slowed down for both processes. In order to examine the effect of reaction time on dye removal, removal efficiencies have been measured between 5 min and 60 min. Color removal efficiencies for n-TiO_2/UV at 5 min were found to be 20.31%, 21.55% and 72.43% at wavelengths of 436, 525 and 620 nm, respectively. Moreover, the removal efficiencies at 5 min in the n-TiO_2/H_2O_2/UV process are 39.38%, 54.70% and 89.04% at 436, 525 and 620 nm wavelengths, respectively. From the 5th to the 60th min, it was observed that the color removal efficiencies increased, but the difference between the color removal efficiencies between 45 min and 60 min were less than about 1% at each wavelength in both processes. Therefore, the 45th min has been determined as the optimum reaction time for both processes.

When both processes are compared, the color removal efficiencies of the n-TiO_2/H_2O_2/UV process are higher than the results obtained with the n-TiO_2/UV process. n-TiO_2/H_2O_2/UV process is a considerable method for the treatment of dyestuffs from wastewater. The highest removal efficiency has been obtained at 620 nm wavelength in the n-TiO_2/UV process. Color removal efficiencies at 436, 525 and 620 nm for 45th min have been obtained as 54.38%, 44.20% and 85.72%, respectively. In addition, the color removal efficiencies that have been achieved at the same wavelengths in the n-TiO_2/H_2O_2/UV process are 90.63%, 92.27% and 99%, respectively, for 45th min. Among the studies examined for dye removal with the n-TiO_2/UV process; more than 90% of the color was removed in 120 min for Methylene Blue [39], in 40 min for Reactive Orange 4 [40], and 45 min for textile wastewater containing Reactive Red 239 [41]. Also, the color removal of Red-147 dye was achieved in 60 min with the n-TiO_2/H_2O_2/UV method, and the treatment efficiency was above 95% [42].

In Table 4, other advanced oxidation studies in the literature examining DB 86, AV 90 and RY 145 dyes alone or in combination with other dyes are examined. Optimum reaction times have been determined as 45 min in both methods used in the study. It has been observed that in Table 4, the processes using catalytic UV, the optimum reaction times vary due to the types of used catalysts to remove only a single dye with a period of 15–240 min. In this study, color removal of synthetic wastewater consisting of a mixture of 3 dyes has been achieved in 45 min.

In addition to the photocatalytic method, other advanced oxidation processes studies involving these dyes are also listed in Table 4. In the advanced oxidation methods presented in Table 4, color removal efficiencies were investigated in optimum parameters such as pH, oxidant doses, catalyst dose, initial concentration, and reaction time. Current study is critical because it is the only study which used n-TiO_2/UV and n-TiO_2/H_2O_2/UV methods with three different color tones as blue, yellow, red are studied together. In the literature, there is no color removal study with advanced oxidation processes containing Direct Blue 86, Reactive Yellow 145 and Acid Violet 90 dyestuffs as a mixture.

3.5. Kinetic analysis of color removal

Kinetic examinations have been used experimental data to obtain reaction rate constants and regression coefficients.

Table 4
Comparison of the current study to previously reported with Direct Blue, Reactive Yellow and Acid Violet dyes

Dyestuff	Treatment method	Optimum conditions	Removal efficiency	References
Direct Blue 86	O_3 UV/O_3	pH 11 100 ppm (initial dye conc.) 35 min	O_3: 99% UV/O_3: 94%	[43]
Direct Blue 86	Photocatalytic treatment with phosphoric acid-based geopolymer	20 W Xenon Lamp 0.3 g of PAG 1:1 50 mg/L (initial dye conc.) 15 min	87.31% with P/Al ratio 1:1	[44]
Direct Blue 129	Photocatalytic treatment with green synthesis of zinc oxide nanoparticles	20 mg/L (initial dye conc.) 0.05 g ZnO visible light irradiation t = 105 min	95%	[45]
Reactive Yellow 14	Photocatalytic oxidation UV/TiO_2	5×10^{-4} mol/L (initial conc.) TiO_2-P25 4 g/L 32 W H_2O_2: 15 mM 20 min	90.4%	[46]
Reactive Yellow 14	UV/TiO_2, UV/H_2O_2 UV/H_2O_2/Fe^{2+} Fe^{2+}/H_2O_2	TiO_2 = 4 g/L $[H_2O_2]$ = 10 mmol/l $[Fe^{2+}]$ = 0.05 mmol/l Irradiation time = 40 min pH: 3	UV/TiO_2 için: 91.3%	[47]
Reactive Yellow 86	UV/TiO_2 UV/TiO_2/BiOCl UV/TiO_2/BiOCl/La_2O_3	120 min	TiO_2: 67% TiO_2/BiOCl: 79% TiO_2/BiOCl/La_2O_3: 92%	[48]
Reactive Yellow 125	Photocatalysis natural zeolite modified with nitrogen-doped TiO_2 photocatalysis (Z-TiO_2-N) UV–Vis irradiation	Photocatalyst = 1 g/L Dye = 25 mg/L pH: 3 240 min	UV/Z-TiO_2-N: 91.6% VIS/Z-TiO_2-N: 94.8%	[49]
Reactive Yellow dye	Photocatalysis	10 mg/L (initial conc.) pH: 3 TiO_2 = 10 mg/L 60 min	UV-TiO_2: 87.5%	[50]
Reactive Yellow 17	Photocatalysis	10 mg/L (initial conc.) $[Fe^{2+}]$ = 0.05 mM $[S_2O_8^{2-}]$ = 1 mM pH: 3 20 min	$S_2O_8^{2-}$/Fe^{2+}: 63.3% O_8^{2-}/UV: 81.0% $S_2O_8^{2-}$/Fe^{2+}/UV: 95.4%	[51]
Reactive Yellow 145 Reactive Orange 122 Reactive Black 5	UV/H_2O_2 Fenton photo-Fenton	50 mg/L (initial conc.) $[H_2O_2]$ = 40 mg/L [Fe] = 1 mg/L pH = 3 and 4	98% for color 60 min 68% for aromatics 60 min 93% for COD 180 min	[52]
Reactive Red 194 Reactive Yellow 145	O_3 H_2O_2/UV-C	Optimum pH = 11 O_3 neutral pH (H_2O_2/UV-C) $[H_2O_2]$ = 40 mM t = 30 min	O_3 process TOC = 43.8% for RY145 35.5% for RR 194 H_2O_2/UV-C process 26.1% for RY145 25.7% for RR 194	[53]
Reactive Red 120 Reactive Black 5 Reactive Yellow 84	UV/H_2O_2	100 mg/L (initial conc.) $[H_2O_2]$ = 24.5 mmol/l Irradiation time = 60 min	Decolorization 99.6%. Mineralization rates were 58.5% for RY84 52.9% for RR84 81.6% for RB5	[54]
Reactive Black 5 Direct Red 28 Direct Yellow 12	UV/H_2O_2/Fe^{2+}	100 mg/L (initial conc.) 16 W low-pressure mercury vapour lamp t = 60 min (UV, UV/H_2O_2) t = 5 min (UV/H_2O_2/Fe^{2+})	UV/H_2O_2 99% for RB5 98% for DY12 in 60 min 70% for DR28 in 120 min UV/H_2O_2/Fe^{2+} 98% for RB5 88% for DY12 85% for DR28 in 5 min	[55]

(Continued)

Table 4

Dyestuff	Treatment method	Optimum conditions	Removal efficiency	References
Acid Violet 7	Ultrasound-H_2O_2	20 mg/L (initial conc.) 40 kHz US 100 W power dissipation pH: 3 [H_2O_2] = 25 ppm t = 180 min	77%	[56]
Acid Violet 7	Ultrasound + Fenton	20 mg/L (initial conc.) 40 kHz US 100 W power dissipation pH: 3 [Fe^{2+}] = 10 ppm [H_2O_2] = 50 ppm t = 2 min	99.9%	[56]
Acid Violet 12	Electrocatalytic oxidation	140 mg/L (initial conc.) 1 A/dm^2 current density pH: 7 Electrolyte concentration of 0.58 g/L t = 30 min	78% COD reduction	[57]
Acid Violet 7	Photocatalytic	0.5 mM (initial conc.) Catalyst [ZnO] = 2 g/L pH: 9 Airflow rate = 8.1 mL/s t = 60 min	99%	[58]
Acid Violet 7	Photo-Fenton	0.5 mM (initial conc.) Fe^{3+} loaded Al_2O_3 UV-A light Catalyst loading of 1 g/L [H_{2O_2}] = 10 mmol Airflow rate = 8.1 mL/s pH: 3 ± 0.1 $I_0 = 1.381 \times 10^{-6}$ Einstein L^{-1} s^{-1} t = 90 min	99%	[59]

R^2 values obtained by kinetic studies show the relationship between reaction rate and time. For this reason, when trying kinetic models, the model with the highest R^2 is preferred. The reaction rate constants obtained are used to determine the concentration of the substances at any time t in the removal of wastewater with this characteristic by the determined method.

In the literature, the reaction rate constant (k) and regression coefficient (R^2) of 4 different kinetic models can be calculated using the reaction time. In this study, k and R^2 values have been calculated based on the reaction time by using four different kinetic models as the first-order, second-order, pseudo-first-order and pseudo-second-order in n-TiO_2/UV and n-TiO_2/H_2O_2/UV processes.

The kinetic equations are given below.

$$\text{First-order kinetic: } \ln\frac{C_o}{C} = kt \tag{14}$$

$$\text{Second-order kinetic: } \frac{1}{C} - \frac{1}{C_o} = kt \tag{15}$$

$$\text{Pseudo-first-order kinetic: } \ln\frac{C_o}{C} = k't \tag{16}$$

$$\text{Pseudo-second-order kinetic: } \frac{t}{C} = \frac{1}{k_2 C_{\max}^2} + \frac{1}{C_{\max}}t \tag{17}$$

where C_o: the initial concentration of dyestuff; C: the dyestuff concentration in t time; C_{max}: the maximum percentage removal efficiency; k: reaction rate constants.

k and R^2 values calculated with 4 different kinetic models for n-TiO_2/UV and n-TiO_2/H_2O_2/UV processes are given in Tables 5 and 6. According to Table 5, pseudo-second-order kinetics for 436, 525 and 620 nm have been determined as the most suitable models because of the highest R^2 in the n-TiO_2/UV process. The k and R^2 values have been calculated as 0.0026 mg/L min and 0.984 at 436 nm, 0.004 L/mg min and 0.986 at 525 nm, and 0.0128 and 0.996 at 620 nm, respectively. Pseudo-second-order kinetic has been found to be the most significant model for the n-TiO_2/H_2O_2/UV process at all wavelengths with the highest $R^{2,}$ as seen in Table 6.

Table 5
R^2 and k values as per kinetic models in TiO_2/UV process

Kinetic model	R^2			k		
	436 nm	525 nm	620 nm	436 nm	525 nm	620 nm
First-order[a]	0.948	0.982	0.909	0.0167	0.0122	0.0467
Second-order[b]	0.979	0.938	0.947	0.0008	0.0004	0.0048
Pseudo-first-order[c]	0.926	0.860	0.854	0.0742	0.0626	0.0817
Pseudo-second-order[b]	0.984	0.986	0.996	0.0026	0.0040	0.0128

[a]k unit: 1/min; [b]k unit: L/mg min, [c]k unit: mg/L min.

Table 6
R^2 and k values as per kinetic models in TiO_2/H_2O_2/UV

Kinetic model	R^2			k		
	436 nm	525 nm	620 nm	436 nm	525 nm	620 nm
First-order[a]	0.947	0.823	0.852	0.0485	0.1108	0.0897
Second-order[b]	0.966	0.966	0.933	0.0059	0.0059	0.0553
Pseudo-first-order[c]	0.937	0.866	0.891	0.2142	0.1769	0.1407
Pseudo-second-order[b]	0.988	0.991	0.996	0.0030	0.0037	0.0186

[a]k unit: 1/min; [b]k unit: L/mg min, [c]k unit: mg/L min.

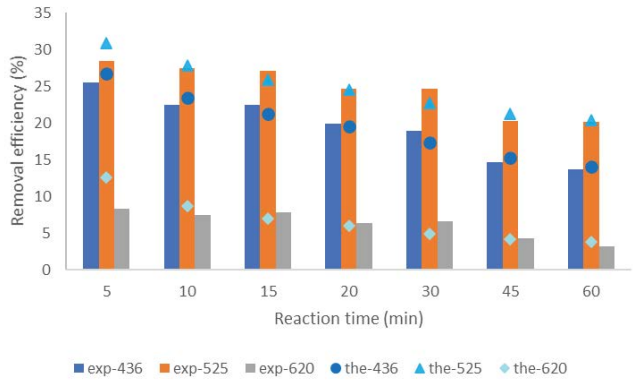

Fig. 7. Theoretical and experimental color removal as second-order kinetics for TiO_2/UV process.

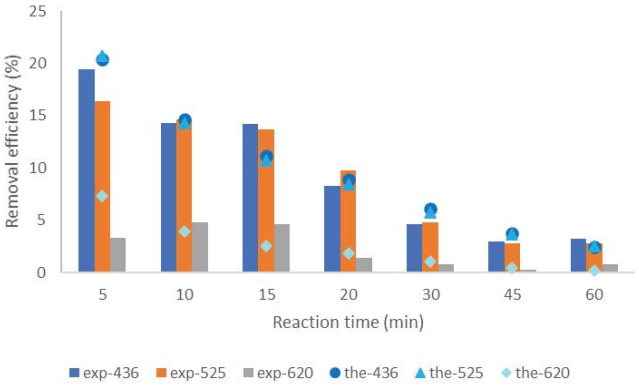

Fig. 8. Theoretical and experimental color removal as second-order kinetics for TiO_2/H_2O_2/UV process.

The k values for 436, 525 and 620 nm wavelengths have been calculated as 0.0030, 0.0037 and 0.0186 L/mg min, respectively, while the R^2 values were calculated as 0.988, 0.991 and 0.996, respectively.

The theoretical color removals have been calculated using the reaction rate constants obtained from the pseudo-second-order model for n-TiO_2/UV and n-TiO_2/H_2O_2/UV processes. Thereafter, the comparison of the theoretical and the experimental results have shown in Fig. 7 for the n-TiO_2/UV process and in Fig. 8 for the n-TiO_2/H_2O_2/UV process. Depending on the results obtained from the calculations at wavelengths of 436 nm, 525 nm and 620 nm, significant results were found that matched the experimental results with the pseudo-second-order model. Figs. 7 and 8 show that except for the theoretical results, especially at 620 and up to 5 min, the theoretical results at the other wavelengths coincide exactly with the experimental results for both processes.

4. Conclusions

Two different processes, n-TiO_2/UV and n-TiO_2/H_2O_2/UV have been researched on the synthetic wastewater containing dyestuffs (DB 86, RY 145 and AV 90) treatment. The effect of pH, n-TiO_2 dose, H_2O_2 dose, and reaction times as operational parameters have been investigated. pH 3, n-TiO_2 125 mg/L and 45 min have been determined as optimum conditions for both processes, and also 750 mg/L H_2O_2 have been found for n-TiO_2/H_2O_2/UV. Under optimum conditions, decolorization efficiencies were 54.38% at 436 nm, 44.20% at 525 nm and 85.72% at 620 nm for the n-TiO_2/UV process, while 90.63% at 436 nm, 92.27% at 525 nm and 99% at 620 nm color removal efficiencies have been achieved in the n-TiO_2/H_2O_2/UV process. While dye removal

was carried out under the same conditions in both processes, when the color removals are examined, the n-TiO_2/H_2O_2/UV process performs much more efficient treatment than the n-TiO_2/UV process. As can be understood from here, it is revealed that hydrogen peroxide advances the treatment efficiency. The results revealed that the pseudo-second-order kinetic model was in concordance with the experimental results for both processes.

References

[1] E.S.B. Ferreira, A.N. Hulme, H. McNab, A. Quye, The natural constituents of historical textile dyes, Chem. Soc. Rev., 33 (2004) 329–336.

[2] Mordor Intelligence Company, Textile Industry – Growth, Trends, COVID-19 Impact, and Forecasts (2021–2026), 2021. Available at: https://www.mordorintelligence.com/industry-reports/global-textileindustry---growth-trends-and-forecast-2019–2024, India (Accessed December 14, 2021).

[3] S.C. Bhatia, Pollution Control in Textile Industry, S. Devraj, Ed., Woodhead Publishing, 2017, India.

[4] T. Setiadi, Y. Andriani, M. Erlania, Treatment of Textile Wastewater by a Combination of Anaerobic and Aerobic Processes: A Denim Processing Plant Case, 6th World Congress of Chemical Engineering, Melbourne, Australia, September 2001.

[5] H.-R. Kariminiaae-Hamedaani, A. Sakurai, M. Sakakibara, Decolorization of synthetic dyes by a new manganese peroxidase-producing white rot fungus, Dyes Pigm., 72 (2007) 157–162.

[6] A. Gürses, M. Açıkyıldız, K. Güneş, M. Sadi Gürses, Classification of Dye and Pigments, in: Dyes and Pigments, 1st ed., Springer, Cham, 2016, pp. 31–45. Available at: https://link.springer.com/book/10.1007/978-3-319-33892-7#about-this-book

[7] S. Benkhaya, S. M'rabet, A. El Harfi, A review on classifications, recent synthesis and applications of textile dyes, Inorg. Chem. Commun., 115 (2020) 107891, doi: 10.1016/J.INOCHE.2020.107891.

[8] N.N. Mahapatra, Textile Dyes and Dyeing, CRC Press, New Delhi, 2016.

[9] S. Shuang, X. Xing, X. Lejin, H. Zhiqiao, Y. Haiping, C. Jianmeng, Y. Bing, Mineralization of CI Reactive Yellow 145 in aqueous solution by ultraviolet-enhanced ozonation, Ind. Eng. Chem. Res., 47 (2008) 1386–1391.

[10] N. Pınar Tanatti, Ş. Türkyilmaz, F. Boysan, İ. Ayhan Şengil, Treatability of textile industry polyester cloth dyeing wastewater by adsorption and photocatalytic method using nTiO_2, Desal. Water Treat., 201 (2020) 452–461.

[11] A. El Nemr, O. Abdelwahab, A. El-Sikaily, A. Khaled, Removal of Direct Blue-86 from aqueous solution by new activated carbon developed from orange peel, J. Hazard. Mater., 161 (2009) 102–110.

[12] N.A. Kalkan, S. Aksoy, E.A. Aksoy, N. Hasirci, Adsorption of Reactive Yellow 145 onto chitosan coated magnetite nanoparticles, J. Appl. Polym. Sci., 124 (2012) 576–584.

[13] L. Bulgariu, L.B. Escudero, O.S. Bello, M. Iqbal, J. Nisar, K.A. Adegoke, F. Alakhras, M. Kornaros, I. Anastopoulos, The utilization of leaf-based adsorbents for dyes removal: a review, J. Mol. Liq., 276 (2019) 728–747.

[14] B. Cojocariu, A. Mihaela Mocanu, G. Nacu, L. Bulgariu, Possible utilization of PET waste as adsorbent for Orange G dye removal from aqueous media, Desal. Water Treat., 104 (2018) 338–345.

[15] B. Shi, G. Li, D. Wang, C. Feng, H. Tang, Removal of direct dyes by coagulation: the performance of preformed polymeric aluminum species, J. Hazard. Mater., 143 (2007) 567–574.

[16] N.N. Patil, S.R. Shukla, Degradation of Reactive Yellow 145 dye by persulfate using microwave and conventional heating, J. Water Process Eng., 7 (2015) 314–327.

[17] C.S. Keskin, A. Özdemir, I. Ayhan Şengil, Simultaneous decolorization of binary mixture of Reactive Yellow and Acid Violet from wastewaters by electrocoagulation, Water Sci. Technol., 63 (2011) 1644–1650.

[18] British Standard Instution, BS EN ISO 7887: 2011 BSI Standards Publication Water Quality—Examination and Determination of Colour, BSI Standards Limited, 2012.

[19] D. Chen, Y. Cheng, N. Zhou, P. Chen, Y. Wang, K. Li, S. Huo, P. Cheng, P. Peng, R. Zhang, L. Wang, H. Liu, Y. Liu, R. Ruan, Photocatalytic degradation of organic pollutants using TiO_2-based photocatalysts: a review, J. Cleaner Prod., 268 (2020) 121725, doi: 10.1016/j.jclepro.2020.121725.

[20] M. Saquib, M. Muneer, Titanium dioxide mediated photocatalyzed degradation of a textile dye derivative, acid orange 8, in aqueous suspensions, Desalination, 155 (2003) 255–263.

[21] I.H. Cho, K.D. Zoh, Photocatalytic degradation of azo dye (Reactive Red 120) in TiO_2/UV system: optimization and modeling using a response surface methodology (RSM) based on the central composite design, Dyes Pigm., 75 (2007) 533–543.

[22] A.E. Amoli, M. Masoumi, M. Sharifzadeh, F. Babaei, G. Firouzzade Pasha, Synthesis of TiO_2-Fe_2O_3 nanocomposite for the photocatalytic degradation of Direct Blue 199 and Basic Yellow 28 dyes under visible light irradiation, J. Dispersion Sci. Technol., (2021) 1–9, doi: 10.1080/01932691.2021.1957924.

[23] N. Areerachakul, S. Sakulkhaemaruethai, M.A.H. Johir, J. Kandasamy, S. Vigneswaran, Photocatalytic degradation of organic pollutants from wastewater using aluminium doped titanium dioxide, J. Water Process Eng., 27 (2019) 177–184.

[24] R. Dhawle, Z. Frontistis, D. Mantzavinos, P. Lianos, Production of hydrogen peroxide with a photocatalytic fuel cell and its application to UV/H_2O_2 degradation of dyes, Chem. Eng. J. Adv., 6 (2021) 100109, doi: 10.1016/j.ceja.2021.100109.

[25] F. Zhang, A. Yediler, X. Liang, A. Kettrup, Effects of dye additives on the ozonation process and oxidation by-products: a comparative study using hydrolyzed C.I. Reactive Red 120, Dyes Pigm., 60 (2004) 1–7.

[26] E.S. Elmolla, M. Chaudhuri, Photocatalytic degradation of amoxicillin, ampicillin and cloxacillin antibiotics in aqueous solution using UV/TiO_2 and UV/H_2O_2/TiO_2 photocatalysis, Desalination, 252 (2010) 46–52.

[27] V. Vatanpour, M. Hazrati, M. Sheydaei, A. Dehqan, Investigation of using UV/H_2O_2 pre-treatment process on filterability and fouling reduction of PVDF/TiO_2 nanocomposite ultrafiltration membrane, Chem. Eng. Process. Process Intensif., 170 (2022) 108677, doi: 10.1016/j.cep.2021.108677.

[28] V.A. Sakkas, P. Calza, M.A. Islam, C. Medana, C. Baiocchi, K. Panagiotou, T. Albanis, TiO_2/H_2O_2 mediated photocatalytic transformation of UV filter 4-methylbenzylidene camphor (4-MBC) in aqueous phase: statistical optimization and photoproduct analysis, Appl. Catal., B, 90 (2009) 526–534.

[29] U.G. Akpan, B.H. Hameed, Parameters affecting the photocatalytic degradation of dyes using TiO_2-based photocatalysts: a review, J. Hazard. Mater., 170 (2009) 520–529.

[30] J. Chang, Q. Zhang, Y. Liu, Y. Shi, Z. Qin, Preparation of Fe3O4/TiO2 magnetic photocatalyst for photocatalytic degradation of phenol, J. Mater. Sci.: Mater. Electron., 29 (2018) 8258–8266.

[31] M. Muruganandham, M. Swaminathan, Photocatalytic decolourisation and degradation of Reactive Orange 4 by TiO_2-UV process, Dyes Pigm., 68 (2006) 133–142.

[32] A. Riga, K. Soutsas, K. Ntampegliotis, V. Karayannis, G. Papapolymerou, Effect of system parameters and of inorganic salts on the decolorization and degradation of Procion H-exl dyes. Comparison of H_2O_2/UV, Fenton, UV/Fenton, TiO_2/UV and TiO_2/UV/H_2O_2 processes, Desalination, 211 (2007) 72–86.

[33] C. Tang, V. Chen, The photocatalytic degradation of Reactive Black 5 using TiO_2/UV in an annular photoreactor, Water Res., 38 (2004) 2775–2781.

[34] A.T. Toor, A. Verma, C.K. Jotshi, P.K. Bajpai, V. Singh, Photocatalytic degradation of Direct Yellow 12 dye using UV/TiO_2 in a shallow pond slurry reactor, Dyes Pigm., 68 (2006) 53–60.

[35] M. Ahmad, M.T. Qureshi, W. Rehman, N.H. Alotaibi, A. Gul, R.S. Abdel Hameed, M. Al Elaimi, M.F.H. Abd el-kader, M. Nawaz, R. Ullah, Enhanced photocatalytic degradation of RhB dye from aqueous solution by biogenic catalyst Ag@ZnO, J. Alloys Compd., 895 (2021) 162636, doi: 10.1016/j.jallcom.2021.162636.

[36] W. Qi, Y. Yang, J. Du, J. Yang, L. Guo, L. Zhao, Highly photocatalytic electrospun Zr/Ag Co-doped titanium dioxide nanofibers for degradation of dye, J. Colloid Interface Sci., 603 (2021) 594–603.
[37] R. Ullah, C. Liu, H. Panezai, A. Gul, J. Sun, X. Wu, Controlled crystal phase and particle size of loaded-TiO_2 using clinoptilolite as support via the hydrothermal method for degradation of crystal violet dye in aqueous solution, Arabian J. Chem., 13 (2020) 4092–4101.
[38] A.P. Naik, H. Mittal, V.S. Wadi, L. Sane, A. Raj, S.M. Alhassan, A. Al Alili, S.V. Bhosale, P.P. Morajkar, Super porous TiO_2 photocatalyst: tailoring the agglomerate porosity into robust structural mesoporosity with enhanced surface area for efficient remediation of azo dye polluted wastewater, J. Environ. Manage., 258 (2020) 110029, doi: 10.1016/j.jenvman.2019.110029.
[39] T. Zhang, T. Oyama, A. Aoshima, H. Hidaka, J. Zhao, N. Serpone, Photooxidative N-demethylation of methylene blue in aqueous TiO_2 dispersions under UV irradiation, J. Photochem. Photobiol., A, 140 (2001) 163–172.
[40] M. Muruganandham, M. Swaminathan, Photocatalytic decolourisation and degradation of Reactive Orange 4 by TiO_2-UV process, Dyes Pigm., 68 (2006) 133–142.
[41] E.M. Saggioro, A.S. Oliveira, T. Pavesi, C.G. Maia, L.F.V. Ferreira, J.C. Moreira, Use of titanium dioxide photocatalysis on the remediation of model textile wastewaters containing azo dyes, Molecules, 16 (2011) 10370–10386.
[42] R. Arshad, T.H. Bokhari, T. Javed, I.A. Bhatti, S. Rasheed, M. Iqbal, A. Nazir, S. Naz, M.I. Khan, M.K.K. Khosa, M. Iqbal, M. Zia-Ur-Rehman, Degradation product distribution of Reactive Red-147 dye treated by UV/H2O2/TiO2 advanced oxidation process, J. Mater. Res. Technol., 9 (2020) 3168–3178.
[43] M.A. Hassaan, A. El Nemr, F.F. Madkour, Testing the advanced oxidation processes on the degradation of Direct Blue 86 dye in wastewater, Egypt. J. Aquat. Res., 43 (2017) 11–19.
[44] L.C. Liu, Y.J. Zhang, H. Chen, P.Y. He, Z.S. Hu, Potential of cost-effective phosphoric acid-based geopolymer as photocatalyst for dye wastewater degradation, Integr. Ferroelectr., An Int. J., 218 (2021) 208–214.
[45] S. Taghavi Fardood, A. Ramazani, S. Moradi, P. Azimzadeh Asiabi, Green synthesis of zinc oxide nanoparticles using arabic gum and photocatalytic degradation of Direct Blue 129 dye under visible light, J. Mater. Sci.: Mater. Electron., 28 (2017) 13596–13601.
[46] M. Muruganandham, M. Swaminathan, TiO_2-UV photocatalytic oxidation of Reactive Yellow 14: effect of operational parameters, J. Hazard. Mater., 135 (2006) 78–86.
[47] M. Muruganandham, M. Swaminathan, Advanced oxidative decolourisation of Reactive Yellow 14 azo dye by UV/TiO_2, UV/H_2O_2, UV/H_2O_2/Fe^{2+} processes – a comparative study, Sep. Purif. Technol., 48 (2006) 297–303.
[48] A. Sridevi, B.R. Ramji, G.K.D. Prasanna Venkatesan, V. Sugumaran, P. Selvakumar, A facile synthesis of TiO_2/BiOCl and TiO_2/BiOCl/La_2O_3 heterostructure photocatalyst for enhanced charge separation efficiency with improved UV-light catalytic activity towards Rhodamine B and Reactive Yellow 86, Inorg. Chem. Commun., 130 (2021) 108715, doi: 10.1016/j.inoche.2021.108715.
[49] E.C. Ilinoiu, R. Pode, F. Manea, L.A. Colar, A. Jakab, C. Orha, C. Ratiu, C. Lazau, P. Sfarloaga, Photocatalytic activity of a nitrogen-doped TiO_2 modified zeolite in the degradation of Reactive Yellow 125 azo dye, J. Taiwan Inst. Chem. Eng., 44 (2013) 270–278.
[50] A. Akshaya, P. Chinnaiyan, D. Unni, G. Keerthana, Use of TiO_2 and rice husk ash to study the removal of Reactive Yellow Dye as contaminant in water, Mater. Today:. Proc., 5 (2018) 24268–24276.
[51] N. Bougdour, A. Sennaoui, I. Bakas, A. Assabbane, Experimental evaluation of Reactive Yellow 17 degradation using UV light and iron ions activated peroxydisulfate: efficiency and kinetic model, Sci. Technol. Mater., 30 (2018) 157–165.
[52] G.E. do Nascimento, D.C. Napoleão, P.K. de Aguiar Silva, R.M. da Rocha Santana, A.M.R. Bastos, L.E.M.C. Zaidan, M.C. de Moura, L.C.B.B. Coelho, M.M.M.B. Duarte, Photo-assisted degradation, toxicological assessment, and modeling using artificial neural networks of Reactive Gray BF-2R dye, Water, Air, Soil Pollut., 229 (2018) 1–15.
[53] S. Gül, Ö. Özcan-Yıldırım, Degradation of Reactive Red 194 and Reactive Yellow 145 azo dyes by O_3 and H_2O_2/UV-C processes, Chem. Eng. J., 155 (2009) 684–690.
[54] M. Neamtu, I. Siminiceanu, A. Yediler, A. Kettrup, Kinetics of decolorization and mineralization of reactive azo dyes in aqueous solution by the UV/H_2O_2 oxidation, Dyes Pigm., 53 (2002) 93–99.
[55] U. Bali, E. Çatalkaya, F. Şengül, Photodegradation of Reactive Black 5, Direct Red 28 and Direct Yellow 12 using UV,UV/H_2O_2 and UV/H_2O_2/Fe^{2+}: a comparative study, J. Hazard. Mater., 114 (2004) 159–166.
[56] S. Kodavatiganti, A.P. Bhat, P.R. Gogate, Intensified degradation of Acid Violet 7 dye using ultrasound combined with hydrogen peroxide, Fenton, and persulfate, Sep. Purif. Technol., 279 (2021) 119673, doi: 10.1016/j.seppur.2021.119673.
[57] N. Mohan, N. Balasubramanian, *In-situ* electrocatalytic oxidation of Acid Violet 12 dye effluent, J. Hazard. Mater., 136 (2006) 239–243.
[58] B. Krishnakumar, M. Swaminathan, Influence of operational parameters on photocatalytic degradation of a genotoxic azo dye Acid Violet 7 in aqueous ZnO suspensions, Spectrochim. Acta, Part A, 81 (2011) 739–744.
[59] I. Muthuvel, M. Swaminathan, Photoassisted Fenton mineralisation of Acid Violet 7 by heterogeneous Fe(III)–Al_2O_3 catalyst, Catal. Commun., 8 (2007) 981–986.